J. Mol. Model. **2000**, *6*, 608 – 617

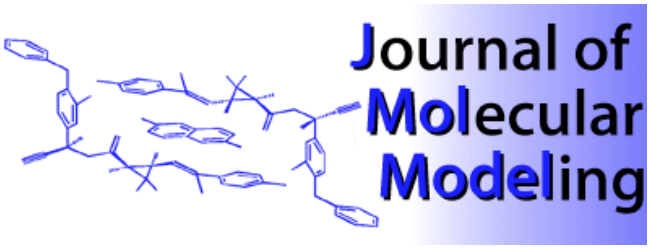

FULL PAPER

Effect of Solvation on Ozonolysis Reaction Intermediates and Transition States

Cenk Selçuki[1],Viktorya Aviyente[1], Philippe Aplincourt[2], and Manuel Felipe Ruiz-López[2]

[1]Chemistry Department, Bogaziçi University, 80815, Bebek, Istanbul, Turkey.

[2]Laboratoire de Chimie théorique, UMR CNRS-UHP No. 7565, Institut Nancéien de Chimie Moléculaire, Université Henri Poincaré-Nancy I, BP 239, F-54506 Vandoeuvre-les-Nancy Cedex, France. Tel: +90-212-2631540 x: 1610; Fax: +90-212-2872467; E-mail: {aviye,selcuki}@boun.edu.tr.

Received: 17 April 2000/ Accepted: 29 June 2000/ Published: 13 December 2000

Abstract Electrostatic solvent effects on the ozonolysis of ethylene have been investigated using correlated *ab initio* and density functional approaches. We use a simple polarizable continuum model for the solvent. It allows us to evaluate the medium effect on both the electronic and nuclear structure of the chemical species involved in the reaction. The computations confirm that basically the reaction proceeds through the Criegee mechanism. However, formation of the van der Waals complexes ethylene/ozone and carbonyl oxide/formaldehyde also appears to play a role. All the calculated species are stabilized with respect to the reactants except the transition state corresponding to the primary ozonide formation. In general, electrostatic solvent effects are relatively small for activation barriers of single reaction steps and more substantial for the corresponding reaction energies. Moreover, the medium significantly modifies the structure of some species for which polarization effects are crucial.

Keywords Ozonolysis, Ozone, Reaction mechanisms, Solvent effects, Theoretical calculations

Introduction

The oxidative cleavage of unsaturated compounds with ozone was first studied in detail by Harries [1] at the beginning of the century. With very few exceptions, a double bond is cleaved quantitatively under extremely mild conditions, usually at or below -78ºC in dilute solutions in the absence of acids and bases. The products of this cleavage were characterized as aldehydes, ketones, their peroxidic derivatives or carboxylic acids, depending on the type of the alkene. Rieche *et al.* [2] observed cyclic peroxides or "ozonides", shown to have the structure of 1,2,4-trioxolanes, as the reaction products of the ozonolysis reaction. In 1958, Criegee and Schröder [3] succeeded to detect primary ozonides experimentally and confirmed the results of Rieche *et al.* Later, Criegee [4, 5] postulated the reaction mechanism now widely accepted in the literature, and confirmed the participation of ozonides. Criegee's mechanism is schematically shown in Figure 1. The first step is the addition of ozone to the carbon-carbon double bond and the formation of the primary ozonide (PO), 1,2,3-trioxolane. In the second step, the primary ozonide decomposes into a carbonyl compound and a carbonyl oxide. The next step is the addition of these two species to form the final ozonide (FO), 1,2,4-trioxolane, that may decompose into different products depending on reaction conditions. The ozonolysis mechanism has been recently

Correspondence to: V. Aviyente

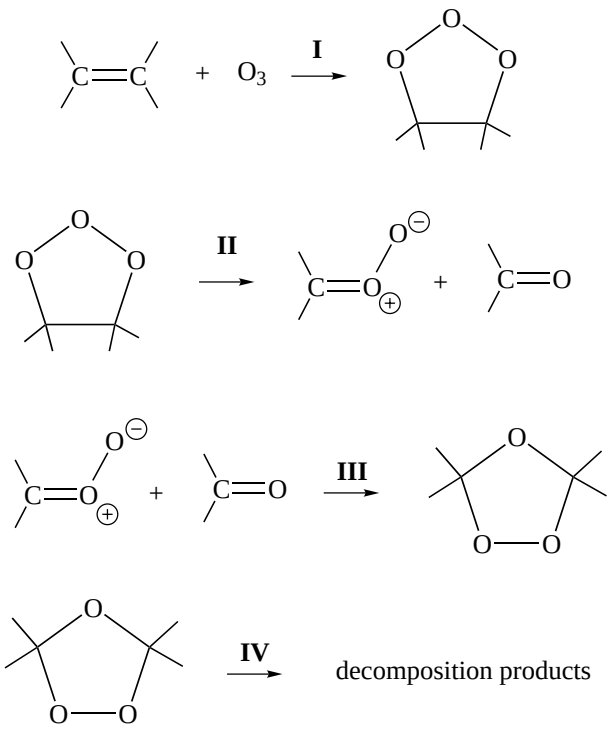

Figure 1 *Schematic Criegee mechanism for ozonolysis*

reviewed [6, 7] and the properties of Criegee intermediates have received some attention (see for instance [8, 9]).

The ozonolysis of alkenes has also been investigated theoretically, most of the investigations being due to Cremer and coworkers [10-14]. In particular, the molecular structure and conformation of primary and final ozonides have been examined by considering ring puckering parameters and employing split-valence and augmented split-valence basis sets [10]. Cremer has found, in contrast to Ruoff's MC-SCF calculations [15, 16], that the most stable structure of PO is the envelope form. Later, McKee [17] confirmed the structure of PO to be an O-envelope and the theoretically predicted geometry was found to be in excellent agreement with the microwave structure [18]. For FO, the twist conformation has been found to be most stable. The ozonolysis of ethylene has indicated that small alkene POs cleave *via* a transition state that favors the formation of a *syn* rather than an *anti* carbonyl oxide [13]. The formation of complexes between ethylene and ozone has been examined at the SCF, MP2 and MP4 (SDTQ) levels of theory with a split-valence-plus-polarization basis. A π-complex has been predicted to be stable [17]. Gillies *et al.* [19] have combined microwave spectra and *ab initio* results to argue that the ozone/ethylene complex lies in a shallow energy minimum along the reaction coordinate. Another π-complex, formed by carbonyl oxide and an aldehyde, has been described by some authors [20-22]. Dewar *et al.* [23] studied the reaction profile of ethylene ozonolysis with AM1 and their results support the Criegee mechanism. Olzmann *et al.* have studied the energetics, kinetics and product distributions of the reactions of ozone with ethene and 2,3-dimethyl butene [24]. Their results have shown that POs are not collisionally stabilized under atmospheric conditions and dissociation of carbonyl oxide intermediates produces OH radicals. Recently, Anglada *et al.* [25] have reinvestigated the gas phase ozonolysis of ethylene including for the first time the decomposition of FO and side reactions of the intermediates.

Most of the computations cited above have assumed isolated molecules and comparison with experiments carried out in solution cannot be made directly. Indeed, the role of solvent effects on the ozonolysis reaction might be important [6]. In particular, the reaction intermediate, carbonyl oxide, is expected to undergo a noticeable solvent effect since it may formally be represented as a combination of diradical and zwitterionic electronic configurations. Indeed, some theoretical studies have been carried out to analyze the role of solvation on the nuclear and electronic structure of this species [22, 26-29]. Del Rio *et al.* [22] have considered the role of solvation on the formation of secondary ozonide from carbonyl oxide and formaldehyde but a complete theoretical study of the ozonolysis reaction in solution is still lacking. The aim of the present work is to achieve such an investigation.

Methodology

The importance of electron correlation has been emphasized in earlier studies for the ozonolysis reaction in the gas-phase [17, 20]. In our study, calculations have been carried out using either the Møller-Plesset approach (MP2 or MP4 (SDQ) [30]) or density functional theory (DFT) with both the restricted and unrestricted formalisms giving the same results. These methods have been chosen as a compromise between computational cost and accuracy, taking into account the conclusion of previous studies. For instance, if one considers the carbonyl oxide species, the results are quite dependent on the theoretical method. At the Hartree-Fock level, the diradical structure is preferred, [31] whereas coupled cluster calculations [32] predict mainly zwitterionic character. The MP2 level overestimates the diradical structure a little [32] but higher-order perturbation corrections do not improve the results much. Besides, Gutbrod *et al.* [33] have demonstrated that density functional calculations at the B3LYP/6-31(d,p) level reproduce the geometrical parameters of carbonyl oxide obtained by CCSDT(T)/TZ+2P calculations [32] and have used this method to optimize geometries.

In MP2 and MP4 calculations, the frozen-core approximation has been used. DFT results have been obtained with the B3LYP exchange-correlation energy functional [34]. The basis set used, 6-31+G(d), is a double zeta one augmented with polarization and diffuse functions on heavy atoms.

To represent the solvent we use the self-consistent reaction field (SCRF) approach developed at Nancy [35-37]. The solvent is simply described as a polarizable dielectric continuum and the solute is placed in a cavity created in this continuum (for details, see the original references). We have

considered the case of a high dielectric medium (ε=78.5) in order to evaluate the upper limit of the electrostatic solvent effect. Obviously, the electrostatic effect of a less polar solvent may be expected to go in the same direction and to be less intense. Note that experimental data in water is available [38, 39], although in such a solvent other effects are expected to take place that would require the explicit consideration of water molecules. A theoretical study of the reaction of carbonyl oxide with a water molecule has been reported elsewhere [40]. In solution, the calculations have been carried out at the MP2/6-31+G(d) level only since the MP4 approach is not available in this case. One should note that, although the MP2 level is probably not very accurate for computing absolute reaction energies (see below however), it is expected to yield suitable predictions for the solvent effect.

Full geometry optimization has been done in the gas phase and in solution and the nature of the structures (minimum or transition state) has been verified as usual using the Hessian matrix eigenvalues. Zero-point energy corrections (ZPE) are estimated in the gas-phase and assumed to be unmodified by the solvent. Calculations were carried out with Gaussian 94 (Revision C.3) [41] and Gaussian 94W (Revision D.3) [41]. The calculations in solution were carried out with the SCRFPAC links [42].

Results and discussion

According to our computations, the ozonolysis of ethylene involves several elemental reaction steps, which confirm the mechanism of Criegee, as summarized in Figure 1. Results in the gas-phase and in a polar medium lead to the same reaction mechanism. However, compared to the schematic mechanism in Figure 1, our computations deserve a few comments. First, we have predicted the formation of a stable complex between ozone and ethylene prior to the formation of the PO. Besides, another complex is predicted between carbonyl oxide and formaldehyde prior to the formation of FO. Finally, for the FO decomposition reaction, we have only investigated a process in which formic acid and formaldehyde are obtained as the final products.

The gas-phase energy profile at different levels is shown in Figure 2. Solvent effects on the reaction profile are dis-

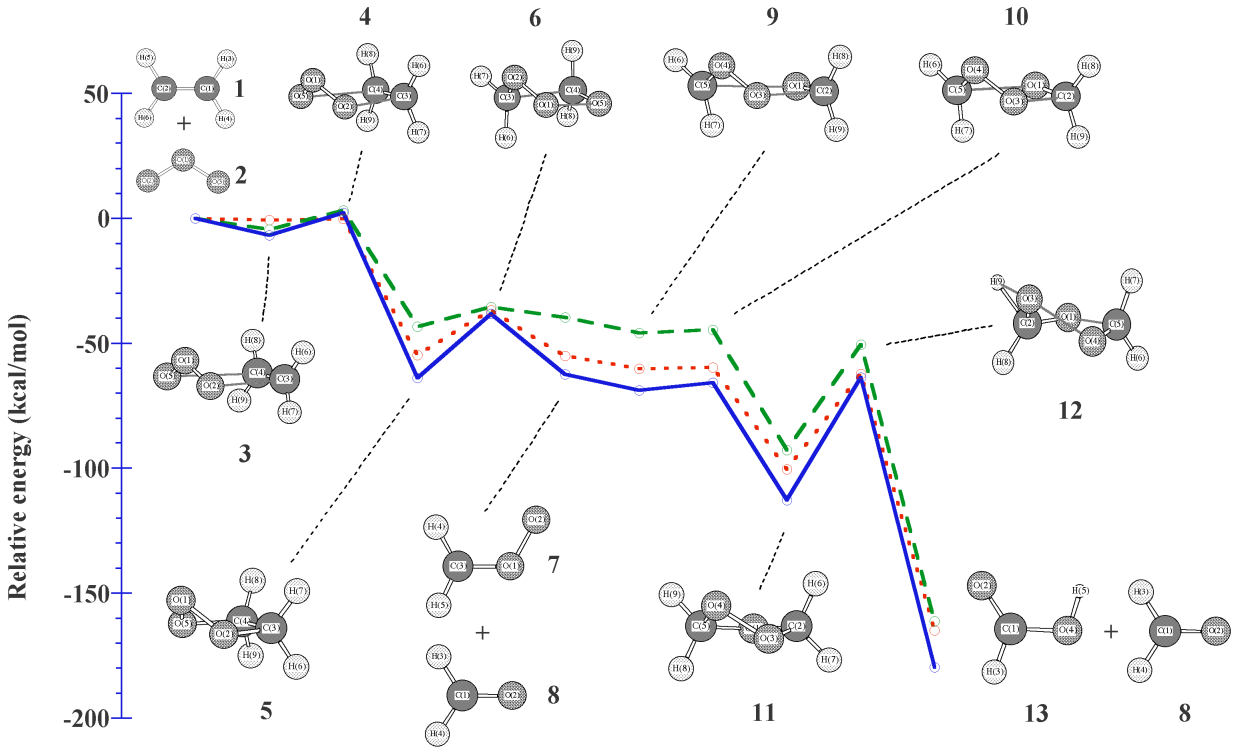

Figure 2 *Predicted reaction profiles in gas phase for ethylene ozonolysis reaction. The curves are computed using MP4 (single), MP2 (dashed) and B3LYP (dotted) approaches*

Table 1 *Calculated parameters for ozone (**1**) and ethylene (**2**) (in Å and degrees)*

	Gas Phase			Solution	
	B3LYP	**MP2**	**MP4 (SDQ)**	**MP2**	**Exp [a]**
ozone					
OO	1.264	1.301	1.270	1.299	1.272
OOO	118.1	116.5	117.7	116.3	116.8
ethylene					
CC	1.335	1.340	1.341	1.342	1.339
CH	1.088	1.086	1.088	1.086	1.086
CCH	121.8	121.6	121.8	121.6	121.2
HCH	116.4	116.8	116.4	116.8	

[a] See References 17 and 43 for ozone, and Reference 17 for ethylene

Table 2 *Calculated parameters for ethylene-ozone complex (**3**) (in Å and in degrees)*

	Gas Phase			Solution
	B3LYP	**MP2**	**MP4 (SDQ)**	**MP2**
OO	1.274	1.332	1.269	1.334
CO	2.705	2.433	3.270	2.413
CC	1.346	1.357	1.341	1.360
OOO	116.4	113.6	117.7	113.2
OOC	96.0	94.2	89.0	94.3
OCC	98.7	100.3	97.3	100.4

Table 3 *Calculated parameters for TS (**4**) (in Å and in degrees)*

	Gas Phase			Solution
	B3LYP	**MP2**	**MP4 (SDQ)**	**MP2**
OO	1.290	1.334	1.298	1.331
CO	2.346	1.990	2.240	2.052
CC	1.364	1.397	1.371	1.390
OOO	113.6	108.4	112.4	109.0
OOC	97.0	97.7	96.4	97.7
OCC	99.8	101.1	100.1	100.9

Table 4 *Calculated parameters for ethylene primary ozonide (**5**) (in Å and in degrees)*

	Gas Phase			Solution	
	B3LYP	**MP2**	**MP4 (SDQ)**	**MP2**	**Exp [a]**
OO	1.446	1.461	1.449	1.462	1.453
CO	1.428	1.434	1.435	1.442	1.417
CC	1.557	1.549	1.549	1.547	1.546
OOO	101.4	100.3	100.7	100.4	100.2
OOC	102.0	101.1	101.3	101.4	102.1
OCC	103.8	104.0	103.7	104.0	103.9

[a] Reference 19

cussed below. The optimized parameters for all the relevant structures in gas-phase and in solution are listed in Table 1 - 11. The experimental values are given where available. For the numbering of the structures, see Figure 2. Relative energies and enthalpies at T=0 K are given in Table 12. Finally, Table 13 summarizes the solvent effect on dipole moments and the solvation energies.

Gas phase results

The whole process may be divided into four steps: formation of PO, decomposition of PO, formation of FO and decomposition of FO. Some of these elementary processes have already been investigated in the gas-phase and our results confirm the reported conclusions [13, 14, 16, 17, 21-23, 25, 43, 44]. Therefore, we describe them very briefly. It may be noted

Table 5 *Calculated parameters for TS (**6**) (in Å and in degrees)*

	Gas Phase			Solution
	B3LYP	**MP2**	**MP4 (SDQ)**	**MP2**
O1O2	1.325	1.289	1.340	1.296
O2C3	1.324	1.354	1.333	1.333
C4C3	1.934	2.276	1.882	2.183
O5C4	1.266	1.255	1.279	1.269
O1O5	2.178	2.267	2.119	2.282
C3O2O1	111.7	116.4	109.7	116.2
C4C3O2	96.9	90.3	97.7	92.1
O5C4C3	102.8	99.2	102.5	100.6
O5O1O2	90.7	90.2	91.4	88.9
C4O5O1	101.3	105.6	101.9	103.6

Table 6 *Calculated parameters for carbonyl oxide (**7**) and formaldehyde (**8**) (in Å in degrees)*

	Gas Phase			Solution
	B3LYP	**MP2**	**MP4 (SDQ)**	**MP2**
carbonyl oxide				
OO	1.356	1.312	1.349	1.390
CO	1.261	1.290	1.270	1.259
CH(syn)	1.088	1.085	1.088	1.086
CH(anti)	1.085	1.081	1.085	1.083
OOC	119.3	119.9	118.8	117.3
OCH(syn)	119.2	118.4	118.7	119.4
OCH(anti)	115.3	114.1	115.1	114.9
HCH	125.5	127.6	126.2	125.8
formaldehyde				
CO	1.209	1.225	1.220	1.231
CH	1.109	1.102	1.105	1.098
OCH	121.9	121.7	121.7	121.4
HCH	116.3	116.6	116.6	117.3

Table 7 *Calculated parameters for carbonyl oxide-formaldehyde dipole complex (**9**) (in Å and in degrees)*

	Gas Phase			Solution
	B3LYP	**MP2**	**MP4 (SDQ)**	**MP2**
O1C2	1.228	1.236	1.229	1.237
O3C2	2.363	2.406	2.519	2.478
O4O3	1.377	1.355	1.379	1.389
C5O4	1.259	1.269	1.260	1.260
O1C5	2.514	2.548	2.629	2.614
O3C2O1	101.6	100.6	100.2	100.0
O4O3C2	94.5	93.7	92.7	94.3
C5O4O3	116.7	117.1	116.8	116.1

in Figure 2 that the energy profiles obtained with the three computational levels employed here (B3LYP, MP2, MP4) are in good qualitative agreement, although the relative energy of some species appear to be quite dependent on the method.

Step I: PO formation (**1**+**2** → **5**): In the first reaction step, ozone (**1**) attacks ethylene (**2**) to form the PO (**5**). The intermediate complex (**3**) was described formerly by McKee *et al.* [17] and is the precursor of the transition structure (TS) (**4**) that leads to PO (**5**). Ozone (**1**) and ethylene (**2**) structures are described adequately with MP2, MP4(SDQ) and B3LYP calculations. Ozone has been confirmed to be a biradical with all the methods and its structure is in good agreement with experiment [45]. The structure calculated for TS (**4**), has C_s symmetry and an envelope-like conformation, with the central oxygen placed out of the plane. The PO (**5**) has an enve-

Table 8 *Calculated parameters for TSIII (**10**) (in Å and in degrees)*

	Gas Phase			Solution
	B3LYP	**MP2**	**MP4 (SDQ)**	**MP2**
O1C2	1.238	1.252	1.256	1.257
O3C2	2.220	2.140	2.091	2.140
O4O3	1.382	1.368	1.393	1.394
C5O4	1.263	1.271	1.270	1.270
O1C5	2.329	2.262	2.166	2.218
O3C2O1	102.3	102.7	103.0	101.7
O4O3C2	94.7	94.7	94.5	95.0
C5O4O3	114.9	114.0	112.1	113.0

Table 9. Calculated parameters for ethylene final ozonide (**11**) (in Å and in degrees).

	Gas Phase			Solution	
	B3LYP	**MP2**	**MP4 (SDQ)**	**MP2**	**Exp [a]**
OO	1.466	1.481	1.467	1.483	1.470
C2O3	1.417	1.422	1.421	1.426	1.395
C2O1	1.422	1.427	1.424	1.430	1.436
COC	104.8	104.4	104.8	104.9	102.8
OCO	105.6	105.6	105.3	105.3	106.3
COO	99.7	98.5	99.1	98.8	99.2

[a] Reference 50

Table 10 *Calculated parameters for TS (**12**) (in Å and in degrees)*

	Gas Phase			Solution
	B3LYP	**MP2**	**MP4(SDQ)**	**MP2**
O1C2	1.296	1.303	1.302	1.315
C2O3	1.341	1.342	1.340	1.331
O4O3	2.023	1.921	1.978	2.385
C5O4	1.265	1.305	1.284	1.325
O1C5	1.877	1.718	1.828	1.621
C2H9	1.208	1.261	1.216	1.271
O3H9	1.516	1.381	1.493	1.389
O3C2O1	117.5	114.5	116.3	113.6
O4O3C2	89.8	91.7	90.0	91.8
C5O4O3	94.3	92.6	94.6	90.4
C5O1C2	97.9	100.0	98.1	102.9
O4C5O1	106.0	108.6	106.6	109.6

lope structure, as also predicted by Cremer's computations [46] and in agreement with the experimental results of Gillies *et al.* [19]. The relative energy (including ZPE) for the formation of the ethylene-ozone complex (see Table 12), is only -0.7 kcal/mol at the B3LYP level whereas it reaches -6.8 kcal/mol at the MP4 level. This substantial difference is probably due to the important role played by dispersion forces in complexation, not accurately predicted by DFT. It is also noteworthy that BSSE (Basis Set Superposition Error) reduces the relative energy of **3** to -6.0 kcal/mol, indicating that this correction has a minor effect on the relative stability of **3** at the MP4 level. Starting from this complex (**3**), the activation barrier to form (**5**) is also dependent on the model. The energy obtained at the MP2 and MP4 levels is in good agreement with the experimental findings (~8 kcal/mol) [47, 48]. The reaction energy in step I (**5**–**3**) is large, reaching -54.0, -38.8 and -57.1 kcal/mol at B3LYP, MP2 and MP4 levels, respectively. The exothermicity of step I has been evaluated with AM1 (-46.0 kcal/mol) [23]. CCSD(T)/6-311G(2d,2p) (-49.2 kcal/mol) [25], HF/4-31G (-41.0 kcal/mol) [44], MP2/6-31G* with unfrozen core (-49.0 kcal/mol) [13] and GVB calculations (-53.0 kcal/mol) [49]. All these values are comparable to ours.

Step II: PO decomposition (**5** → **7** + **8**): This step involves the cleavage of the PO (**5**) into carbonyl oxide (**7**) and formaldehyde (**8**). In the corresponding TS (**6**), one may note that the O1O2, O2C3 and C4O5 bond lengths are relatively

Table 11 *Calculated parameters for formic acid (**13**) (in Å and in degrees)*

	Gas Phase			Solution
	B3LYP	**MP2**	**MP4 (SDQ)**	**MP2**
C1O2	1.207	1.217	1.212	1.223
C1O4	1.348	1.354	1.352	1.347
CH	1.098	1.095	1.097	1.094
OH	0.978	0.982	0.980	0.984
O4C1O2	125.1	125.0	125.0	124.9
O4C1H3	109.4	109.8	110.0	110.3
C1O4H5	107.8	107.1	107.4	108.5
O2C1H3	125.1	125.2	125.0	124.8

Table 12 *Relative energies (kcal·mol^{-1}) for the ozonolysis of ethylene. Values in paranthesis include zero point corrections*

	Gas Phase						Solution	
	B3LYP		**MP2**		**MP4 (SDQ)**		**MP2**	
1 + **2**	0.0	(0.0)	0.0	(0.0)	0.0	(0.0)	0.0	(0.0)
Step I								
3	-2.0	(-0.7)	-6.0	(-4.5)	-2.3	(-6.8)	-6.0	(-4.5)
4	-1.7	(-0.1)	2.5	(3.3)	5.6	(2.3)	3.5	(4.3)
Step II								
5	-59.8	(-54.7)	-47.0	(-43.3)	-64.1	(-63.9)	-50.4	(-46.7)
6	-39.4	(-36.7)	-36.3	(-35.4)	-35.9	(-38.2)	-40.3	(-39.4)
7 + **8**	-54.8	(-55.0)	-37.7	(-39.6)	-56.6	(-62.3)	-48.4	(-50.4)
Step III								
9	-62.0	(-60.1)	-46.3	(-45.8)	-65.2	(-68.8)	-52.1	(-51.6)
10	-61.9	(-59.7)	-45.9	(-44.6)	-63.3	(-65.7)	-51.0	(-49.7)
Step IV								
11	-106.4	(-100.4)	-97.4	(-92.6)	-114.0	(-112.8)	-99.7	(-94.9)
12	-62.8	(-62.2)	-50.1	(-50.5)	-59.2	(-63.6)	-53.5	(-53.9)
8 + **13**	-166.1	(-164.8)	-161.0	(-161.2)	-175.7	(-179.6)	-167.4	(-167.7)

Table 13 *MP2 results for dipole moments and solvation energies of the studied structures*

	Dipole Moment (D)		E_{SOLV}
	Gas Phase	**Solution**	**(kcal/mol) [a]**
1	0.00	0.00	-1.0
2	0.81	0.94	-0.6
3	1.36	2.13	-1.6
4	4.81	6.62	-0.6
5	4.14	5.09	-5.0
6	6.56	9.15	-5.7
7	5.82	7.60	-8.8
8	3.08	3.80	-3.5
9	2.79	3.76	-7.4
10	2.73	3.93	-6.7
11	1.27	1.53	-3.9
12	2.93	4.93	-5.1
13	1.71	2.22	-4.6

[a] $E_{SOLV} = E_{ELEC}(Solution) - E_{ELEC}(Gas)$

short whereas C3C4 and O1O5 distances are large. Thus, this TS has late character. The energy barrier is much higher than that for step I, as pointed out earlier [13]. Besides, step II is endothermic.

Step III: FO formation (**7** + **8** → **11**): Species **7** and **8** may form an intermediate complex (**9**) which has already been described through MP4 (SDQ)/6-31G(d,p) [20]. All the methods used here have allowed to locate this stationary point and predict complexation energies in the range 5-8 kcal/mol. Note that in complex (**9**), the molecular dipole moments are aligned in antiparallel way leading to dipole-dipole attraction. From the complex, the species undergo a cycloaddition reaction forming FO (**11**) through a small energy barrier. Indeed, the fact that carbonyl oxide intermediates in ozonizations can be efficiently trapped [50] suggests that there must be a barrier to recombination of (**7**) and (**8**), in agreement with our results.

The geometry of TS (**10**) corresponds to a distorted envelope leading to maximum orbital overlap. Actually, the ge-

ometry of (**10**) is very similar to that of complex (**9**) explaining that activation energies are rather small. All the methods lead to a C2O3 bond length around 2.1 Å and O1C5 bond length around 2.2 Å. The structure for FO (**11**) agrees quite well with previous theoretical results [10, 11]. Compared to experimental results of Gillies and Kuczkowski [50], the C2O3 bond is overestimated by all the methods. For the O1C2 bond, the situation is reversed and all the methods used underestimate its length. Hence, our computations predict a more symmetric structure for FO than that found experimentally.

Step IV: FO decomposition (**11** → **8** + **13**): Several reactions may be envisaged for the decomposition of FO. In particular, formic acid anhydride has been detected in atmospheric conditions [51]. A theoretical study of the corresponding process has been reported [52]. Here, as pointed out above, we focus on the decomposition of (**11**) in formaldehyde (**8**) and formic acid (**13**). Such a process occurs via migration of hydrogen accompanying ring cleavage. As seen in Figure 2, hydrogen has partially migrated to O3 in the TS (**12**), the C2H9 bond length has increased to 1.26 Å and the O3H9 distance has shortened to 1.38 Å. The O3O4 (1.92 Å) and the O1C5 (1.72 Å) bond lengths indicate that the O3O4 bond has cleaved to a greater extent. Step IV is highly exothermic (68.6 kcal/mol at MP2 level), the transition state is early but the activation barriers are substantial (the order of magnitude is 40-50 kcal/mol).

Solvent effects

All the species located in gas-phase have also been found in solution. Recently, it has been shown that the energies of activation of 1,3-dipolar cycloadditions are larger in solution than in the gas phase, whereas the reaction energies are lower [53]. This has been explained by the higher solvation energies of the 1,3-dipoles. Cossío *et al.* [53] have indicated that the large zwitterionic character of 1,3-dipoles diminishes along the reaction coordinate, thereby resulting in lower solvation energies for the transition structures and the reaction products. During the addition of ozone (**2**) to ethylene (**1**), the activation barrier increases in solution by 1 kcal/mol as expected (Table 12). However, in contrast to the results of Cossío *et al.* [53], the exothermicity of the reaction increases by 3.4 kcal/mol due to the higher stabilization of the primary ozonide (**5**) in solution. It is noteworthy that the complex formed by carbonyl oxide and formaldehyde (**9**) remains stable in solution. This is an interesting result since one could expect the separated species to be more stable. Indeed, the solvation energy of **7** + **8** (-12.3 kcal/mol) is significantly larger than that for complex **9** (-7.4 kcal/mol). However, this trend is not able to reverse the relative stability in the gas phase (**9** is more stable by 6.2 kcal/mol at the MP2 level with ZPE corrections). According to this, one may hypothesize that in solution the PO decomposition does not necessarily lead to the separated species **7** + **8**. These two species could rearrange in the solvent cage [54] to yield **9,** which is slightly more favorable energetically. Obviously, the continuum model employed here prevents us giving a definitive conclusion on this point. That would require solvent dynamics to be taken into account.

Let us consider the modifications induced by the solvent on the geometric and electronic structures of reaction intermediates and transition states. Medium effects on the geometry of some intermediates have already been described in our previous work [22, 26]. In particular, a large effect has been pointed out for the carbonyl oxide **7** due to an increase of its zwitterionic character in presence of a polar medium [22, 26-29]. Such a large effect is confirmed here. The highest change appears for the OO distance, which increases by almost 0.08 Å (see Table 6). The effect is accompanied by a large polarization, as shown by the value of the dipole moment in Table 13. In Table 13, one also sees that carbonyl oxide exhibits the largest solvation energy of all the species along the reaction path. One may then expect that these structural modifications of the carbonyl oxide influence its chemical properties substantially. For instance, the double bond character in C=O-O changes with solvation. These consequences of such effects on reaction energetics are commented below.

The solvent effect is also important in species like the complex **9**, where the C2O3 bond length increases by 0.07 Å. Another interesting trend is the decrease of the OO bond length in ozone by 0.03 Å which may be interpreted as due to a weight increase of the zwitterionic structures $O{=}O^{+}{-}O^{-}$.

Let us now consider in some detail the transition structures **4**, **6**, **10** and **12**. All the transition structures are substantially polarized by the solvent (for example, the induced dipole moment of **6** is as large as 2.59 D). The main geometrical change for TS **4** is the lengthening of the CO bond by 0.05 Å, the structure being therefore more reactant-like than in gas phase. For TS **6**, the main change is the large increase of the CC bond length (0.07 Å), which is one of the bonds being broken. The other coordinate directly implied in the reaction coordinate is the O1O5 length. It also increases through the solvent effect but the change is smaller (0.02 Å). Thus, the transition state is in this case closer to the products and the reaction is advanced by the solvent, the effect also increasing the asymmetry of this structure. Other changes in **4** are the lengthening of the O1O5 (0.02 Å) and C4O5 (0.01 Å) bonds and the shortening of the O2C3 bond (0.02 Å). In TS **10**, the distances of the bonds being formed are shortened, especially that for the O1C5 bond (0.04 Å) so that the reaction is advanced, too. Finally, for TS **12**, the main change is for the O1C5 bond, which is shorter in solution (0.06 Å). All the other parameters directly involved in the reaction coordinate (C2H9, O3H9, O3O4) are lengthened more or less by 0.01 Å.

Considering now the energetics of the process (see Tables 12 and 13), one notes that the solvation energies for **7**, **9** and **10** are the most important ones. The activation energies for steps I and III slightly increase (by 1.0 kcal/mol and 0.7 kcal/mol respectively) whereas those for step II and IV slightly decrease (by 0.6 kcal/mol and 1.1 kcal/mol respectively). The effect on reaction energies is much more pronounced. The formation of PO, is more exothermic by 3.4 kcal/mol. In step

II, the reaction energy increases in absolute value by 7.3 kcal/mol and in step III the reaction energy decreases by 8.4 kcal/mol. Finally, step IV is more exothermic by 4.2 kcal/mol. If one considers the global process ethylene (**1**) + ozone (**2**) → FO (**11**), the exothermicity increases a little, by 2.3 kcal/mol. The increase is larger if one considers, as final products, formaldehyde **8** and formic acid **13** (6.5 kcal/mol).

Conclusion

A theoretical study of the Criegee mechanism for the ozonolysis of ethylene in solution has been reported here. Such a reaction had already been studied by different authors but neglecting the role of the solvent. Our results confirm the main reaction steps, in which two van der Waals complexes, not generally considered in the literature, are also involved. The activation barriers of the elementary steps are not fundamentally different from those for the gas phase reaction and this explains why previous theoretical studies with isolated systems lead to plausible conclusions. This result is due to the fact that the solvation energies for the different transition states are very close to those for the corresponding precursors, which is not surprising considering their similar structures in the four reaction steps. Conversely, the individual step reaction energies change notably whereas the whole reaction exothermicity is increased by 6.5 kcal/mol. Besides, the medium effect is quite large concerning the structures of the species. The zwitterionic nature of several species is as expected favored and the transition states in solution display notable differences with respect to gas phase structures.

The relative energies in solution of the species (**6**), (**7**+**8**) and (**9**), suggest that a cage reaction mechanism, already suggested for ozonolysis reactions [53], cannot be excluded. Indeed, the separation of the carbonyl oxide and carbonyl compound does not seem to be in general more favorable than the recombination within a cage created by the solvent. In this work we did not succeed to find a transition state joining (**5**) and (**9**) directly but the existence of such a structure cannot be completely discarded. The main problems to solve in order to achieve a definitive conclusion are related to the computational level and solvent model. Improving them represents a substantial increase of the computational cost, especially considering the fact that solvent dynamic effects are probably important. Such a question is however interesting and merits further research efforts.

Acknowledgements This work is supported by the Bogaziçi University Research Funds (Project number 98B504D). Cenk Selçuki acknowledges the hospitality of the Laboratoire de Chimie théorique during his stay in Nancy.

References

1. Harries, C. *Liebigs Ann. Chem.* **1905**, *343*, 311.
2. Rieche, A.; Meister, R.; Sauthoff, H. *Liebigs Ann. Chem.* **1942**, *553*, 246.
3. Criegee, R.; Schršder, G. *Chem Ber.* **1960**, *93*, 689.
4. Criegee, R. *Chimia* **1968**, *22*, 392.
5. Criegee, R. *Angew. Chem.* **1975**, *87*, 765; Criegee, R. *Angew. Chem. Int. Ed.* **1975**, *14*, 745.
6. Kuczkowski, R. L. *Chem. Soc. Reviews* **1992**, 79.
7. Horie, O.; Moortgat, G. *Acc. Chem. Res.* **1998**, *31*, 387.
8. Nori, M.; Tabuchi, T.; Nojima, M.; Kusabayashi, S. *J. Org. Chem.* **1992**, *57*, 1649.
9. Neeb, P.; Horie, O.; Moortgat, G. *Chem. Phys. Lett.* **1995**, *246*, 150.
10. Cremer, D. *J. Chem. Phys.* **1979**, *70*, 1898.
11. Cremer, D. *J. Am. Chem. Soc.* **1979**, *101*, 7199.
12. Cremer, D.; Gauss J. *Chem. Phys. Lett.* **1989**, *163*, 549.
13. Cremer, D. *J. Am. Chem. Soc.* **1981**, *103*, 3627.
14. Cremer, D. *J. Am. Chem. Soc.* **1981**, *103*, 3633.
15. Ruoff, P.; Almlöf, T.; Saebo, S. *Chem. Phys. Lett.* **1980**, *72*, 489.
16. Ruoff, P.; Saebo, S.; Almlöf, T. *Chem. Phys. Lett.* **1981**, *83*, 549.
17. McKee, M. L.; McMichael Rohlfing, C. *J. Am. Chem. Soc.* **1989**, *111*, 2497.
18. Zozom, J.; Gillies, C. W.; Suenram, R. D.; Lovas, F. J. *Chem. Phys. Lett.* **1987**, *139*, 64.
19. Gillies, C. W.; Gillies, J. Z.; Suenram, R. D.; Lovas, F. J.; Kraka, E.; Cremer, D. *J. Am. Chem. Soc.* **1991**, *113*, 2412.
20. Cremer, D.; Kraka, E.; McKee, M. L.; Radhakrishnan, T. P. *Chem. Phys. Lett.* **1991**, *187*, 491.
21. Ponec, R.; Yuzhakov, G.; Haas Y.; Samuni, U. *J. Org. Chem.* **1997**, *62*, 2757.
22. Del Rio, E.; Aplincourt, P.; Ruiz-López, M. F. *Chem. Phys. Lett.* **1997**, *280*, 444.
23. Dewar, M. J. S.; Hwang, J. C.; Kuhn, D. R. *J. Am. Chem. Soc.* **1991**, *113*, 735.
24. Olzmann, M.; Kraka, E.; Cremer, D.; Gutbrod, R.; Andersson, S. *J. Phys. Chem.* **1997**, *101*, 9421.
25. Anglada, J. M.; Crehuet, R.; Bofill, J. M. *Chem. Eur. J.* **1999**, *5*, 1809.
26. Selçuki, C.; Aviyente, V. *Chem. Phys. Lett.* **1998**, *288*, 669.
27. Steinke, T.; Hansele, E.; Clark, T. *J. Am. Chem. Soc.* **1989**, *111*, 9107.
28. Sola, M.; Lledos, A.; Duran, M.; Bertran, J. *Int. J. Quantum Chem.* **1991**, *40*, 511.
29. Parrondo, R. M.; Karafiloglou, P.; Pappalardo, R. R.; Marcos, E. S. *J. Phys. Chem.* **1995**, *99*, 6461.
30. (a) Møller, C.; Plesset, M. S. *Phys. Rev.* **1934**, *46*, 618; (b) Pople, J. A.; Binkley, J. S.; Seeger, R. *Int. J. Quantum Chem. Symp.* **1980**, *10*, 1; (c) Krishnan, R.; Pople, J. A. *Int. J. Quantum Chem.* **1978**, *14*, 91; (d) Krishnan, R.; Frisch, M. J.; Pople, J. A. *J. Chem. Phys.* **1980**, *72*, 4244.
31. Kahn, S. D.; Hehre, W. J.; Pople, J. A. *J. Am. Chem. Soc.* **1987**, *109*, 1871.
32. Cremer, D.; Gauss, J.; Kraka, E.; Stanton, J. F.; Bartlett, R. J. *Chem. Phys. Lett.* **1993**, *209*, 547.
33. Gutbrod, R.; Schindler, R. N.; Kraka, E.; Cremer, D. *Chem. Phys. Lett.* **1996**, *252*, 221.

34. (a) Becke, A. D. *J. Chem. Phys.* **1993**, *98*, 5648; (b) Lee, C.; Yang, W.; Parr, R. G. *Phys. Rev. B 41*, **1988**, 785.
35. Rivail, J. L.; Rinaldi, D.; Ruiz-López, M. F., In *Theoretical and computational models for organic chemistry;* Formosinho, S. J.; Csizmedia, I. G.; Arnaut, L.; Eds.;NATO ASI Series C, Kluwer: Dordrecht, 1991; Vol. 339, pp 79-92.
36. Rinaldi, D.; Rivail, J. L.; Rguini, N. *J. Comput. Chem.* **1992**, *13*, 675.
37. Dillet, V.; Rinaldi, D.; Angyan, J. G.; Rivail, J. L. *Chem. Phys. Lett.* **1993**, *202*, 18.
38. Gäb, S.; Turner, W. V.; Wolff, S.; Becker, K. H.; Ruppert, L.; Brockmann, K. J. *Atmos. Environ.* **1995**, *29*, 2401.
39. Thamm, J.; Wolff, S.; Turner, W. V.; Gäb, S.; Thomas, W.; Zabel, F.; Fink, E. H.; Becker, K. H. *Chem. Phys. Lett.* **1996**, *258*, 155.
40. Aplincourt, P.; Ruiz-López, M. F. submitted.
41. (a) Frisch, M. J.; Head-Gordon, M.; Trucks, G. W.; Foresman, J. B.; Schlegel, H. B.; Raghavachari, K.; Robb, M. A.; Binkley, J. S.; Gonzales, C.; Defrees, D. J.; Fox, D. J.; Whiteside, R. A.; Seeger, R.; Melius, C. F.; Baker, J.; Martin, R. L.; Kahn, L. R.; Stewart, J. J. P.; Topiol, S.; Pople, J. A. Gaussian 94, Gaussian Inc., Pittsburgh, PA, 1994; (b) Frisch, M. J.; Trucks, G. W.; Schlegel, H. B.; Gill, P. M. W.; Johnson, B. J.; Robb, M. A.; Cheeseman, J. R.; Keith, T.; Petersson, G. A.; Montgomery, J. A.; Raghavachari, K.; Al-Laham, M. A.; Zakrzewski, V. G.; Ortiz, J. V.; Foresman, J. B.; Cioslowski, J.; Stefanov, B. B.; Nanayakkara, A.; Challacombe, M.; Peng, C. Y.; Ayala, P. Y.; Chen, W.; Wong, M. W.; Andres, J. L.; Replogle, E. S.; Comperts, R.; Martin, R. L.; Fox, D. J.; Binkley, J. S.; Defrees, D. J.; Baker, J.; Stewart, J. J. P.; Head-Gordon, M.; Gonzales, C.; Pople, J. A. Gaussian 94, Gaussian Inc., Pittsburgh PA, 1995.
42. Rinaldi, D.; Papalardo, R. R. SCRFPAC: QCPE, Indiana University: Bloomington, IN, 1992: Program number 622. Adapted version for Gaussian 94 by D. Rinaldi.
43. Samuni,U.; Haas,Y. *Spectrochimica Acta Part A* **1996**, *52*, 1479.
44. Hiberty, P.C.; Devidal, J. P. *Tetrahedron* **1979**, *35*, 1015.
45. Tanaka, T.; Morino, Y. *J. Mol. Spectrosc.* **1979**, *33*, 538.
46. Cremer, D. *J. Chem. Phys.* **1979**, *70*, 1911.
47. DeMore, W. B. *Int. J. Chem. Kinet.* **1969**, *1*, 209.
48. Adenji, S. A.; Kerr, J. A.; Williams, M. R. *Int. J. Chem. Kinet.* **1981**, *13*, 209.
49. Harding, L. B.; Goddard III, W. A. *J. Am. Chem. Soc.* **1978**, *100*, 7180.
50. Gillies, C. W.; Kuczkowski, R. L. *J. Am. Chem. Soc.* **1972**, *94*, 6337.
51. Su, F.; Calvert, J. G.; Shaw, J. H. *J. Phys. Chem.* **1980**, *84*, 239.
52. Aplincourt, P.; Ruiz-López, M. F. *J. Phys. Chem.* A **2000**, *104*, 380.
53. Cossío, F. P.; Morao, I.; Jiao, H.; Schleyer, Pvr. *J. Am. Chem. Soc.* **1999**, *121*, 6737.
54. Reichardt, C. *Solvent effect in Organic Chemistry*; Verlag Chemie: New York, 1979; p. 182.